1921

Low temperature epitaxial $NiSi_2$ formation on Si(111) by diffusing Ni through amorphous Ni–Zr

R. de Reus, H. C. Tissink, and F. W. Saris
FOM-Institute for Atomic and Molecular Physics, Kruislaan 407, 1098 SJ Amsterdam, The Netherlands

(Received 5 June 1989; accepted 25 September 1989)

Although amorphous alloys are known to be good diffusion barriers, amorphous nickel-zirconium is shown to react with Si at relatively low temperatures. Diffusion of Ni at 350 °C through an amorphous Ni–Zr buffer layer leads to the formation of epitaxial $NiSi_2$ on single crystal silicon substrates. Interplay of mobility and thermodynamics is applicable for epitaxial silicide nucleation and growth. Also, a one-step annealing process in oxygen ambient leads to bilayer formation of $NiSi_2/ZrO_2$ structures on silicon substrates.

I. INTRODUCTION

Many amorphous alloys consisting of near noble and refractory metal atoms have been shown to react with silicon at temperatures around 600 °C.[1] Diffusion couples of near noble metals and silicon usually react around 300 °C, at which temperature the near noble metal is the moving species. In amorphous alloys, however, the near noble metal is locked in the amorphous matrix and unable to react with the silicon substrate.[1] At the reaction temperature of silicon and the refractory metal, a refractory metal silicide will be formed and the near noble metal will be released to form a silicide, too. In this process Si is the moving species, which becomes mobile at around 600 °C.

There is a special class of amorphous metal alloys in which near noble metal atoms are mobile. In fact, amorphous metal alloys can be formed by a solid state reaction starting with multilayers or bilayers of the pure elements.[2] For instance, amorphous Ni–Zr (*a*–NiZr) is formed by the diffusion of Ni not only in Zr, but also in the *a*–NiZr.[3,4] Thus it is expected that in such amorphous alloys the near noble metal atom is mobile enough to react with Si at relatively low temperatures. It is the purpose of this paper to show that this is indeed the case.

II. EXPERIMENTAL

Amorphous $Ni_{60}Zr_{40}$ films with a thickness of 400 Å were codeposited in a dual electron gun evaporator onto Si(111) single crystal substrates. On top of this structure 250 Å Ni was deposited. The base pressure of the deposition system was less than 2×10^{-6} Pa. The silicon substrates were etched in a 4% HF solution prior to deposition. Following deposition the samples were annealed in a furnace in a vacuum better than 6×10^{-6} Pa at temperatures between 250 and 600 °C.

In a second series of experiments on Si(111) *a*–$Ni_{40}Zr_{60}$ was evaporated and the sample was annealed in oxygen ambient.

Analysis of the samples was performed using 2 MeV $^4He^+$ Rutherford backscattering spectroscopy (RBS) and x-ray diffraction (XRD) of Cu Kα radiation in a conventional Θ-2Θ geometry. For a third analysis method, transmission electron microscopy (TEM), a special set of samples was prepared. Onto freshly cleaved single crystal NaCl substrates first a 100 Å thick amorphous Si layer was deposited, followed by a 200 Å thick *a*–$Ni_{60}Zr_{40}$ film. On part of the samples an additional 100 Å thick Ni top layer was deposited. After dissolving the NaCl substrates in de-ionized water, the samples were mounted onto molybdenum TEM grids.

For the study of the Si(111)/*a*–NiZr/Ni sample structures a composition of 60 at.% Ni was chosen for the amorphous alloy. This composition is the most stable amorphous phase. Crystallization temperatures as high as 600 °C are reported.[5,6] Also, it is close to the final composition for *a*–NiZr formed by a solid state reaction.[3] This high stability allows diffusion of Ni through the *a*–NiZr into the silicon substrate. The high crystallization temperature allows annealing at elevated temperatures; thereby the diffusivity is increased without crystallization of the *a*–NiZr layer.

First the results of vacuum annealing will be presented, then the effect of annealing in oxygen ambient.

A. Vacuum annealing

1. Results

Amorphous phase formation of Ni–Zr has been observed[3,9] below 275 °C, in which process Ni is the moving species. However, in the Si(111)/*a*–$Ni_{60}Zr_{40}$/Ni samples no changes were observed after 44 h annealing at this temperature. At 350 °C reaction occurs. In Fig. 1 the Ni and Zr parts of normal RBS spectra of unreacted and reacted samples are plotted. The surface peak positions for Ni and Zr are indicated. The silicon substrate is not shown in these spectra. In the spectrum of the as-deposited sample we see the Ni top layer at

 © 1990 Materials Research Society

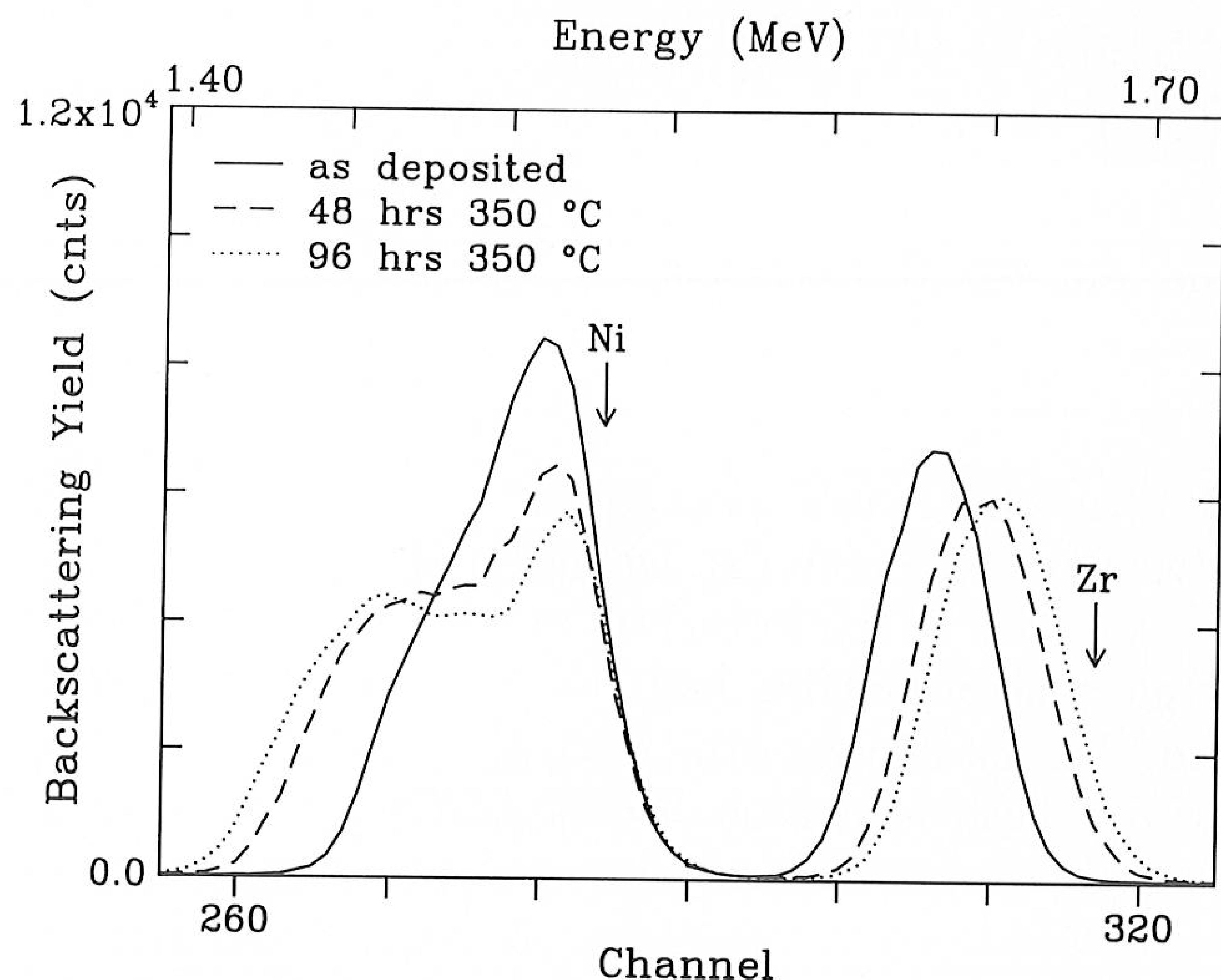

FIG. 1. 2 MeV $^4He^+$ RBS spectra of Si(111)/a–$Ni_{60}Zr_{40}$/Ni samples before and after reacting. Sample tilt 7°, scattering angle 165°. Surface channels are indicated with arrows.

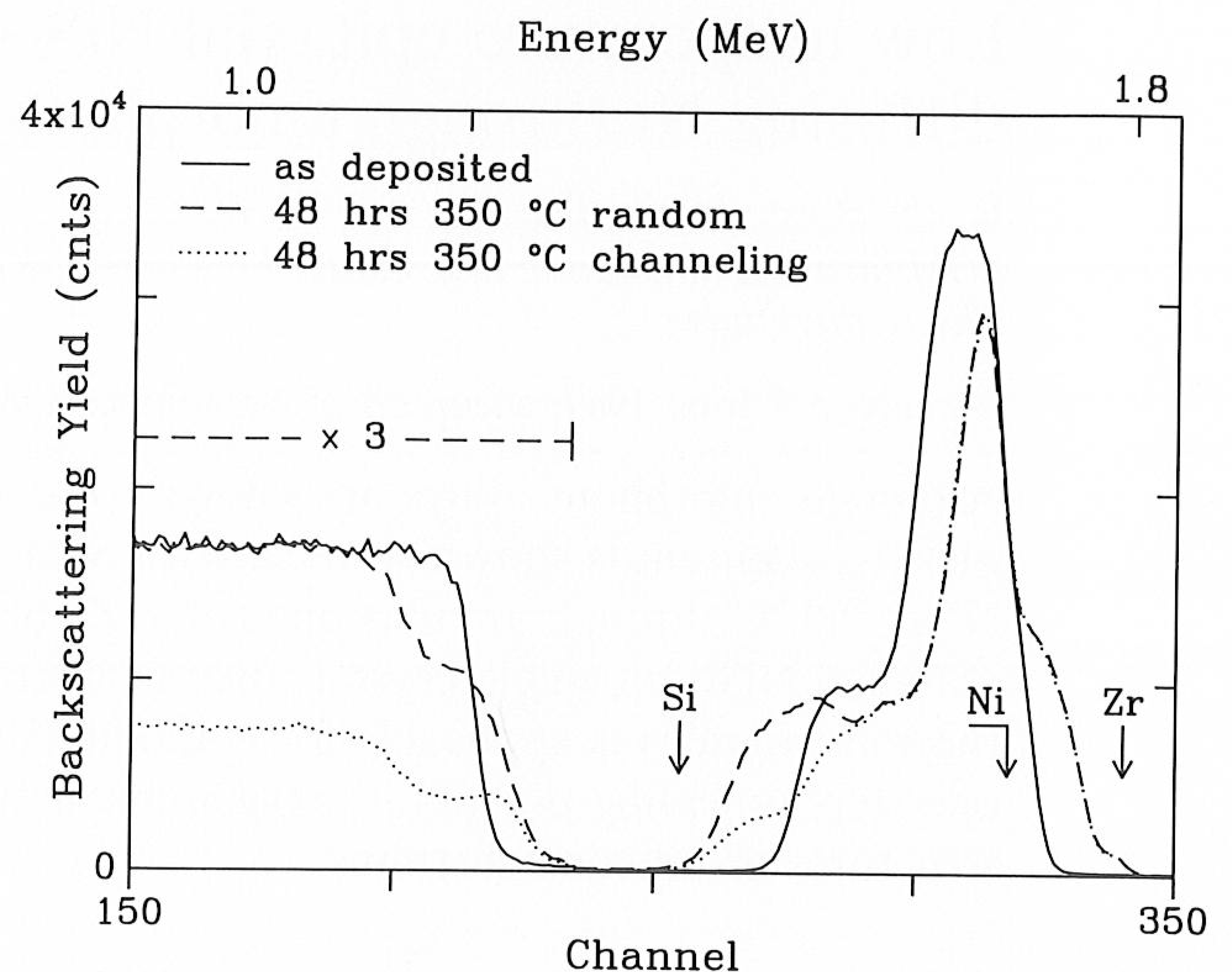

FIG. 2. RBS spectra of samples as in Fig. 1. Scattering angle is 105°. Sample tilt for the random spectra was 7°. Channeling is observed along the ⟨111⟩ surface normal.

the surface position, and the Ni of the a–NiZr appears as a shoulder in the trailing edge. The Zr signal, arising from Zr in the a–NiZr under the Ni top layer, is clearly shifted to lower energies with respect to the surface peak position. The spectrum after annealing the sample at 350 °C for 48 h clearly shows that reaction has occurred. The Ni signal of the top layer has decreased and Ni has penetrated into the sample, as can be seen by a broadening of the signal at the low energy side of the Ni peak. The Zr peak shape has hardly changed, but it has moved toward the surface, as expected. After annealing 96 h at 350 °C, the reaction has proceeded further. The Ni surface signal has decreased again and the Zr peak appears rather close to the surface; its shape is still almost identical compared to the case after 48 h annealing. Ni has penetrated deeper into the sample and three layers may be distinguished: first, the peak of the pure Ni at the surface; second, a plateau of Ni in the a–NiZr; and third, the Ni which has reacted with the Si substrate.

The reaction with the Si substrate may be better observed in Fig. 2. RBS spectra were collected at glancing exit angles for increased depth resolution. We compare the Si signal in the spectrum of the as-deposited sample with the spectrum after annealing 48 h at 350 °C. A plateau is observed, indicating reaction of Si with the metal overlayer. Although the metal peaks overlap, the reaction of Ni also is clearly noticeable.

From analysis of the RBS spectra with the RUMP computer code[10] it is concluded that after the 48 h annealing the initial 250 Å thick Ni top layer has decreased to a thickness of 120 Å. The composition of the reacted Ni–Si layer points toward $NiSi_2$ formation. The thickness of this layer is 500 Å. For formation of this layer just as much Ni is consumed as has disappeared from the Ni top layer. The initial 400 Å thick a–$Ni_{60}Zr_{40}$ buffer layer did not change upon reaction. After 96 h at 350 °C, the thickness of the Ni top layer has decreased to 80 Å and the thickness of the $NiSi_2$ layer has increased to 700 Å. The a–$Ni_{60}Zr_{40}$ layer remained unchanged.

If $NiSi_2$ is formed, it may be epitaxial with the Si(111) substrate. This was tested by channeling analysis. The channeling spectrum of the sample annealed 48 h, also shown in Fig. 2, confirms the formation of an epitaxial $NiSi_2$ layer. The yield in the RBS spectra in the surface region of Si and in the substrate region of Ni is reduced because of channeling in the epitaxial layer.

Additional information for characterization of phases appearing in the samples has been obtained by XRD. Figure 3 shows the most important features of the

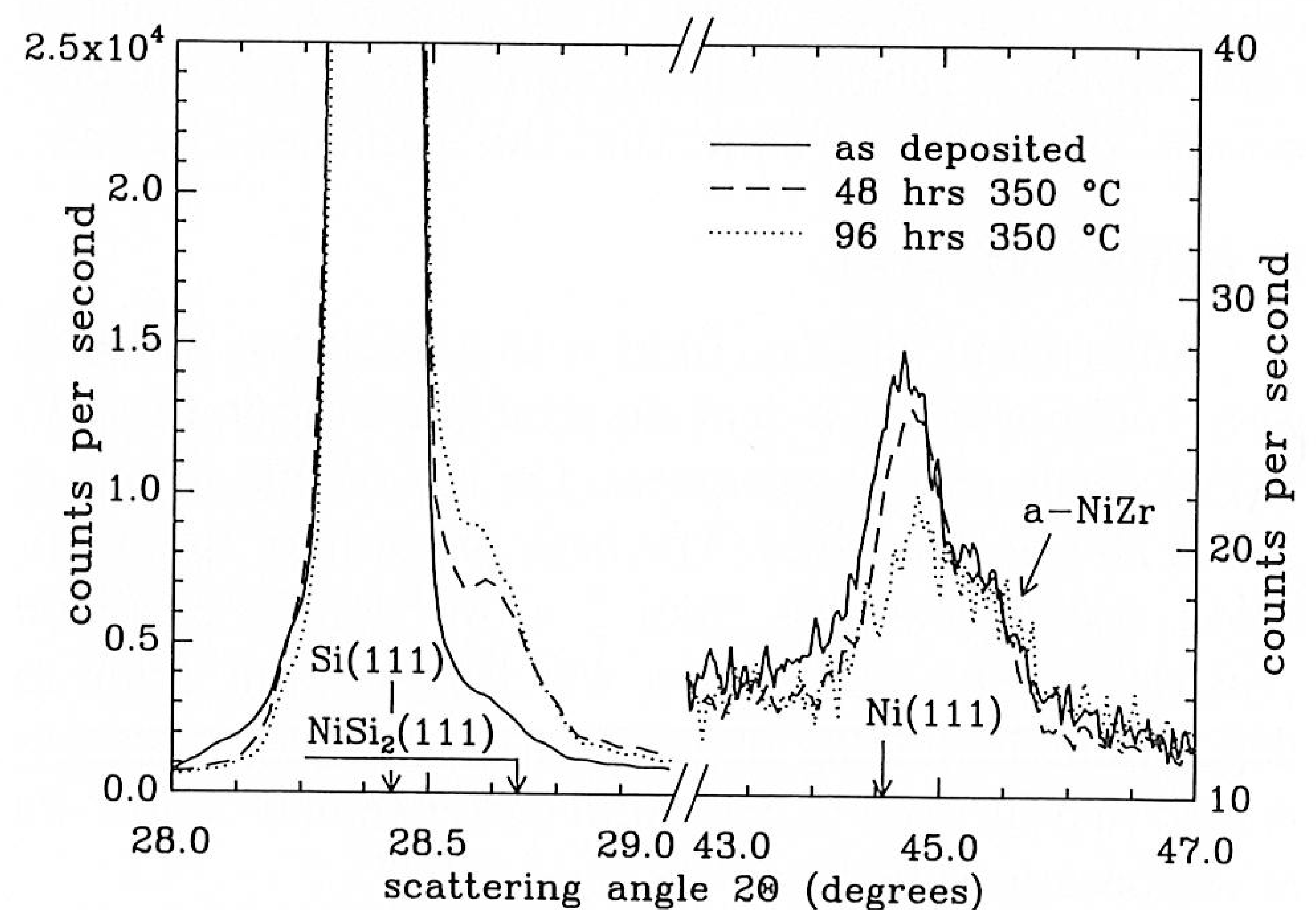

FIG. 3. XRD spectra of Si(111)/a–$Ni_{60}Zr_{40}$/Ni samples, showing the formation of epitaxial $NiSi_2$ and a decrease of the Ni reflection. The broad peak of the a–$Ni_{60}Zr_{40}$ remains unchanged.

XRD spectra before and after reaction. The spectrum of the as-deposited sample shows reflections only of the Si substrate, the Ni top layer, and a broad feature of the *a*–NiZr. After annealing at 350 °C for 48 and 96 h, a decrease of the Ni reflection is observed. At the same time the $NiSi_2$(111) reflection appears. These results confirm the interpretation of the RBS measurements. From this it is concluded that at 350 °C Ni is diffusing through the *a*–$Ni_{60}Zr_{40}$ layer and epitaxial $NiSi_2$ is formed at the Si(111)/*a*–NiZr interface.

Results obtained by TEM show the same behavior for *a*–Si/*a*–$Ni_{60}Zr_{40}$/Ni samples. This is shown in the micrographs at the left-hand side of Fig. 4. The right-hand side shows the results for *a*–Si/*a*–$Ni_{60}Zr_{40}$ samples without Ni top layer. In the micrographs of the as-deposited samples the fine-grained Ni top layer [Fig. 4(a)] and the structureless *a*–Si/*a*–NiZr [Fig. 4(e)] are visible in bright-field image. In the diffraction patterns two broad halos are observed, arising from the *a*–Si and *a*–NiZr. In addition, Ni lines of the Ni top layer are visible in Fig. 4(a). After annealing for 1 h at 350 °C, no changes are observed in the sample without the Ni top layer [Fig. 4(f)], whereas small crystals of Ni_2Si in random orientation are observed in case the extra Ni layer is present [Fig. 4(b)]. Again, no changes are observed in the *a*–Si/*a*–NiZr samples after annealing at 400 °C for 1 h [Fig. 4(g)]. However, randomly oriented $NiSi_2$ is observed and the *a*–Si has disappeared in the *a*–Si/*a*–NiZr/Ni samples [Fig. 4(c)], the same as after annealing at 350 °C for 12 h [Fig. 4(d)]. Finally, Fig. 4(h) shows that after annealing 12 h at 350 °C reaction also occurs in the *a*–Si/*a*–NiZr samples. In this case $NiSi_2$ is formed at the cost of breaking up the *a*–NiZr to release Ni for the reaction, leaving behind the metastable β–Zr phase. Two lines in the diffraction pattern remain unidentified.

These results show that $NiSi_2$ is readily formed if a Ni layer is present on top of the *a*–Si/*a*–NiZr structure. Formation of $NiSi_2$ seems to be frustrated if there is no additional Ni top layer present. This is even more pronounced if the *a*–Si substrate is replaced by Si(111). RBS measurements on Si(111)/*a*–$Ni_{40}Zr_{60}$ samples are presented in Fig. 5. Isochronal annealing for 1 h does not result in reactions up to 500 °C. At 600 °C, which is above the crystallization temperature of *a*–$Ni_{40}Zr_{60}$, reaction is observed and both $ZrSi_2$ and NiSi are identified (also by XRD, not shown). No other phases are observed. Note in Fig. 5 that the slope of the Ni trailing edge and the silicon signal after reacting indicate very rough interfaces.

2. Discussion

Our measurements convincingly show diffusivity of Ni through an *a*–$Ni_{60}Zr_{40}$ layer at 350 °C and the formation of epitaxial $NiSi_2$. The growth of the silicide layer follows a square root time dependence. The *a*–NiZr diffusion barrier limits the growth of the silicide. Therefore, we can estimate the diffusivity of Ni through the *a*–NiZr, using the growth rate of the silicide. From the relation $x = \sqrt{Dt}$, in which x is the silicide layer thickness and t the annealing time, we obtain $D \approx 1.4 \times 10^{-16}$ cm^2/s. Indeed, in *a*–NiZr a Ni diffusion coefficient in the range of 10^{-16} cm^2/s has been found.[3,11] Interdiffusivity of Ni and Si is much faster; see, for instance, Ref. 12. This indicates that the growth of the silicide layer is controlled by the diffusivity in the *a*–NiZr layer. The very slow supply of Ni to the silicide that is formed, and hence the long annealing times, allows the Ni–Si system to reach thermodynamic equilibrium. In Ni–Si diffusion couples the normal sequence in phase formation for annealing times up to a few hours is as follows.[13,14] The first phase formed, from RT to approximately 350 °C, is Ni_2Si. Above 350 °C NiSi is formed. Both phases grow in a layer-by-layer fashion. Near 700 °C $NiSi_2$ is formed by a heterogeneous nucleation process. Apparently, the supply of Ni at 350 °C at a very slow rate through *a*–NiZr allows nucleation of the silicon-rich $NiSi_2$ phase. The absence of fast diffusion paths in the *a*–NiZr, like grain boundaries, results in a homogeneous supply of Ni at the Si/*a*–NiZr interface. As a consequence of this, the interfaces of the silicide formed during reaction are sharp. At higher temperatures, e.g., 400 °C, the reaction rate is much higher. In this case nucleation of $NiSi_2$ is suppressed, the formation of NiSi is observed, and the interfaces become rough.

Our TEM observations indicate differences in reactivity for the different systems studied. Without a Ni top layer the reactivity in our samples is much reduced. Reactions appear to occur easier in the *a*–Si/*a*–NiZr/Ni samples than where crystalline silicon is involved. This difference has also been observed in other studies.[15] We can explain these differences by taking a closer look at the energy balance of the different reactions. We approximate the Gibbs free energies of the phases by their enthalpies, because the entropy term in the solid phase is small. For the reactions observed, the following reaction enthalpies are obtained:

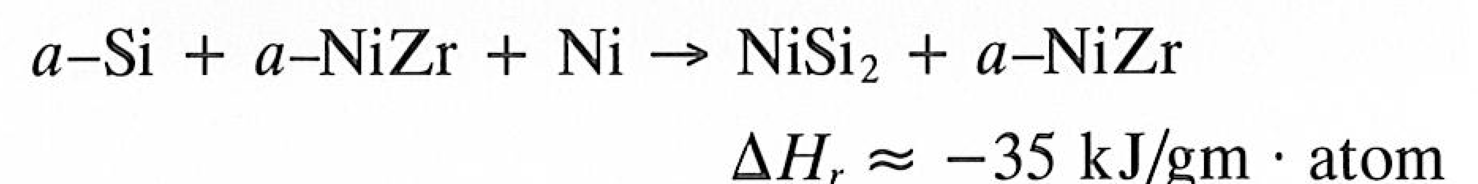

$$a\text{–Si} + a\text{–NiZr} + \text{Ni} \rightarrow \text{NiSi}_2 + a\text{–NiZr} \qquad \Delta H_r \approx -35 \text{ kJ/gm} \cdot \text{atom}$$

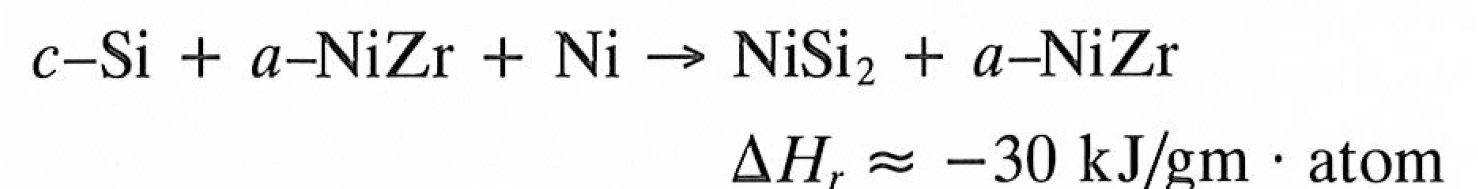

$$c\text{–Si} + a\text{–NiZr} + \text{Ni} \rightarrow \text{NiSi}_2 + a\text{–NiZr} \qquad \Delta H_r \approx -30 \text{ kJ/gm} \cdot \text{atom}$$

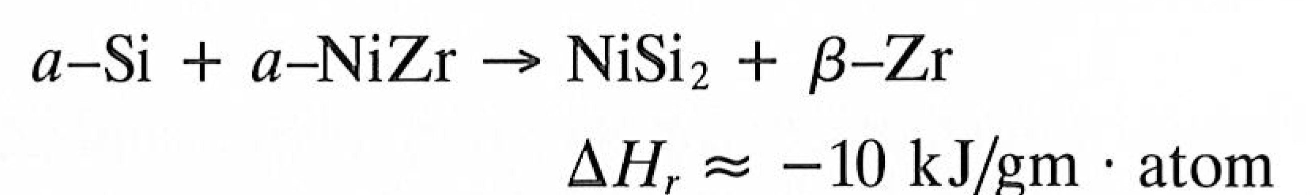

$$a\text{–Si} + a\text{–NiZr} \rightarrow \text{NiSi}_2 + \beta\text{–Zr} \qquad \Delta H_r \approx -10 \text{ kJ/gm} \cdot \text{atom}$$

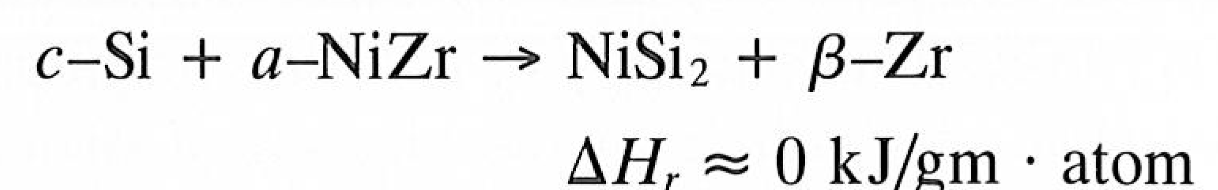

$$c\text{–Si} + a\text{–NiZr} \rightarrow \text{NiSi}_2 + \beta\text{–Zr} \qquad \Delta H_r \approx 0 \text{ kJ/gm} \cdot \text{atom}$$

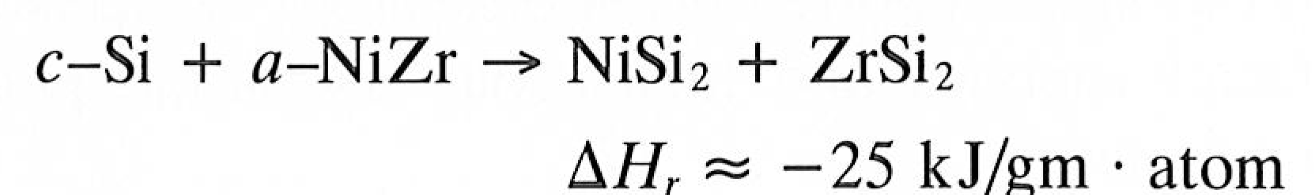

$$c\text{–Si} + a\text{–NiZr} \rightarrow \text{NiSi}_2 + \text{ZrSi}_2 \qquad \Delta H_r \approx -25 \text{ kJ/gm} \cdot \text{atom}$$

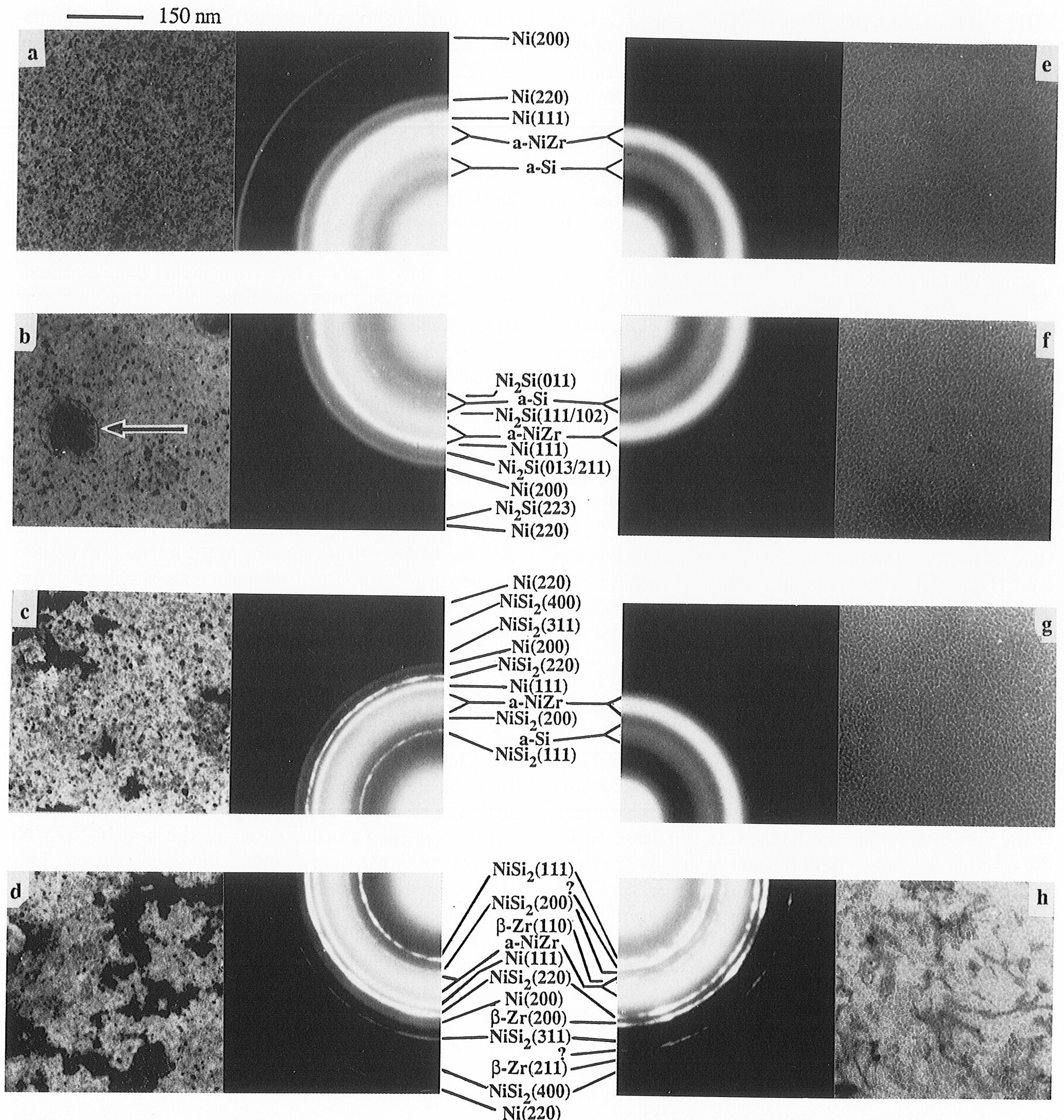

FIG. 4. Bright-field images and selected area diffraction patterns of a–Si/a–$Ni_{60}Zr_{40}$/Ni samples [left-hand side, (a)–(d)] and a–Si/a–$Ni_{60}Zr_{40}$ samples [right-hand side, (e)–(h)] obtained by TEM. Pictures are taken after deposition (a) and (e), after 1 h annealing in vacuum at 350 °C (b) and (f), after 1 h annealing at 400 °C (c) and (g), and after 12 h annealing at 350 °C (d) and (h). The arrow in (b) indicates a Ni_2Si crystal.

Heats of formation for a–NiZr, $NiSi_2$, and $ZrSi_2$ are taken from Refs. 7, 8, and 14. Calorimetric values for the crystallization enthalpy of a–Si are between 10 and 15 kJ/mole, depending on the amount of structural relaxation, as reported by Roorda *et al.*[16] Effects of interfacial energies and metastable crystalline phases are neglected.

In the presence of the Ni top layer the energy gain is due to nickel silicide formation at the expense of Ni consumption. This reaction is highly exothermic. Where amorphous silicon is present, the system also benefits the additional crystallization energy of the a–Si. Without the Ni top layer silicides can be formed only at the expense of breaking up the a–NiZr. Reacting a–NiZr with

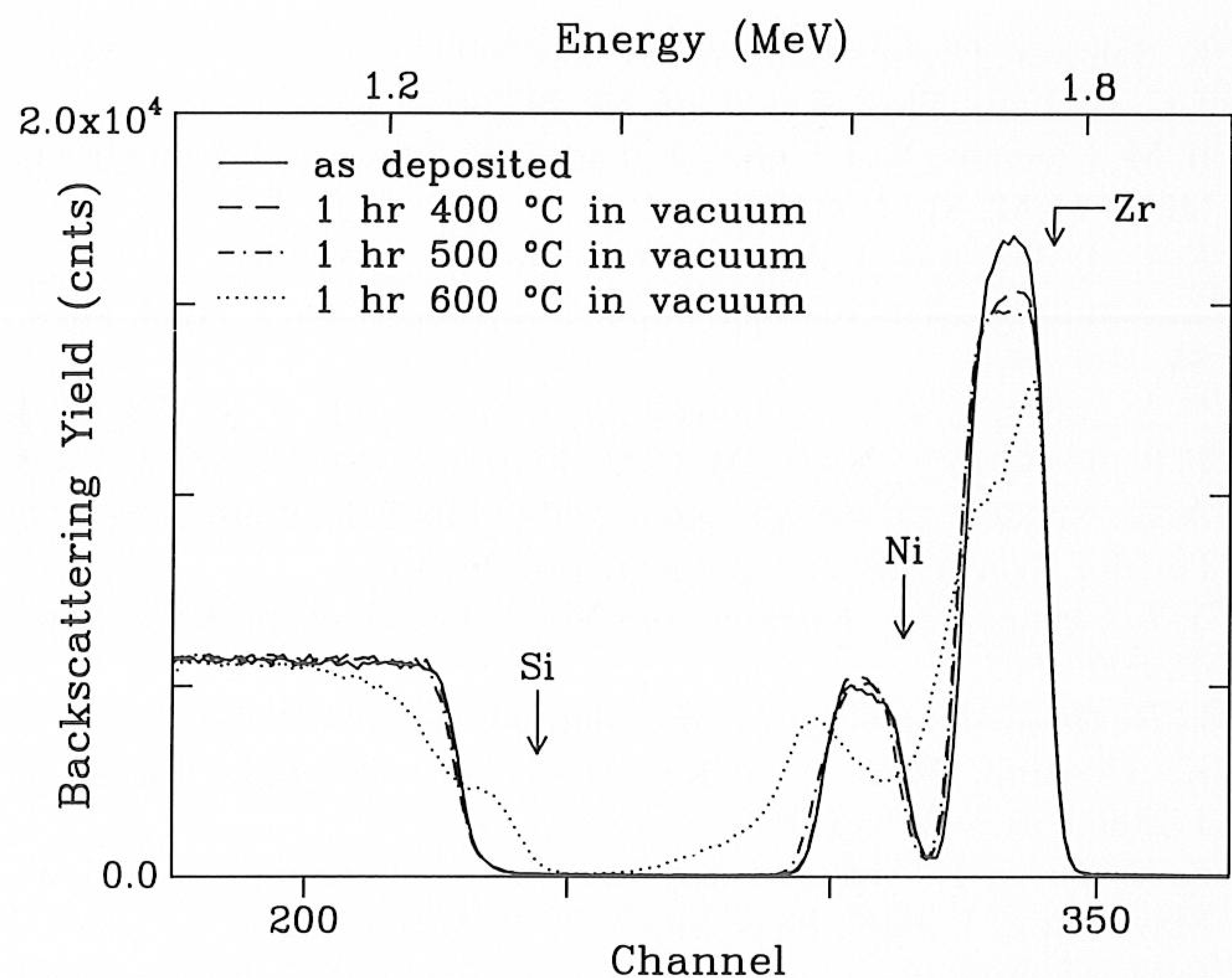

FIG. 5. RBS spectra of vacuum annealed Si(111)/a–$Ni_{40}Zr_{60}$ samples obtained by 2 MeV $^4He^+$. Sample tilt 7°, scattering angle 115°.

a–Si at 350 °C still is an exothermic process, whereas the heat of reaction is 0 when c–Si is used. Only if $ZrSi_2$ can be formed, at 600 °C, can the system gain energy and reactions will proceed, as observed in Fig. 5.

B. Annealing in oxygen ambient

Results and discussion

Si(111)/a–$Ni_{40}Zr_{60}$ samples were also annealed under oxygen flow. In Fig. 6 the results after annealing the sample for 2 h at 500 °C in an oxygen pressure of 10^{-4} mbar are shown. In the spectrum of the as-deposited sample both Ni and Zr are present at the sample surface. After annealing a large amount of oxygen is detected. The oxygen has reacted with the Zr to form polycrystalline ZrO_2, also confirmed by XRD. The

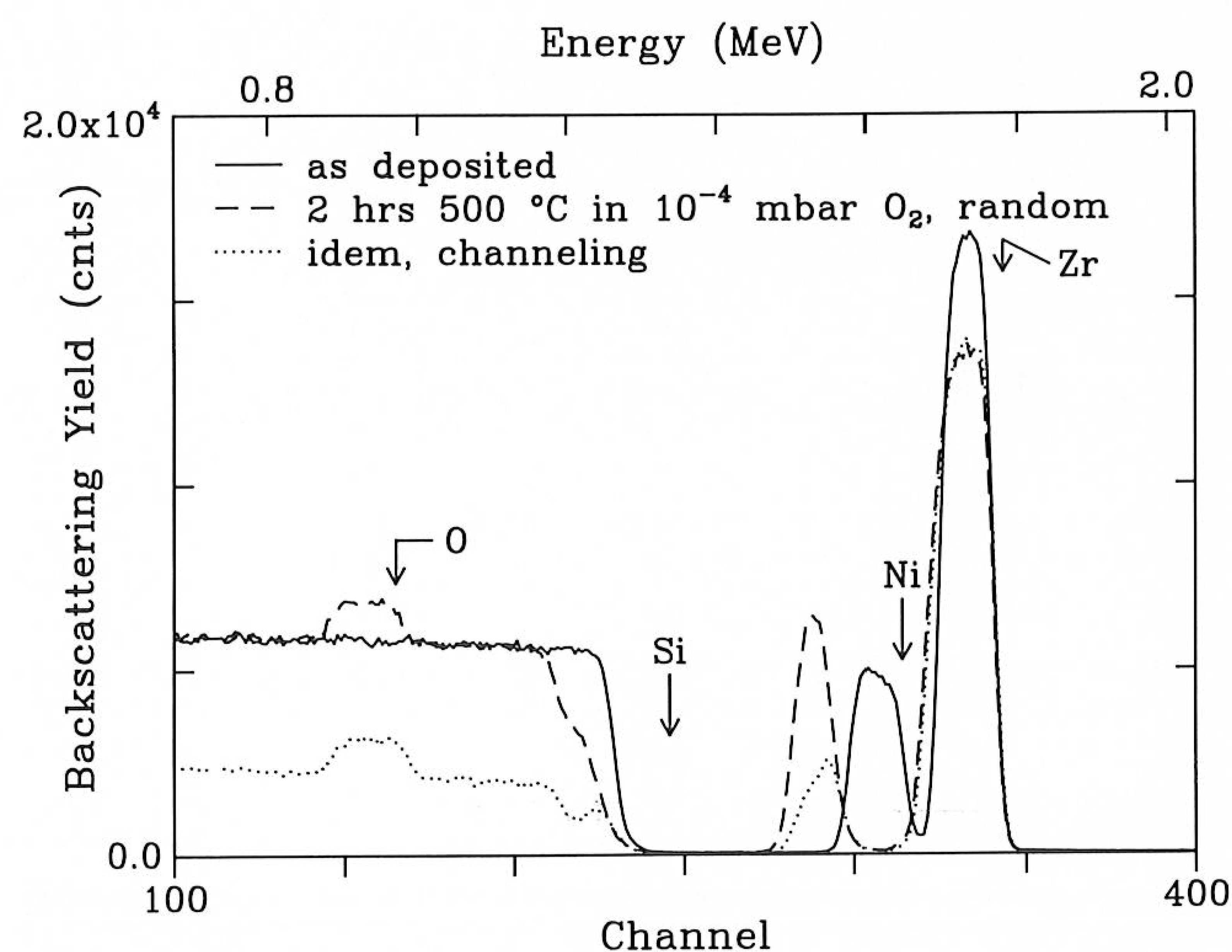

FIG. 6. RBS spectra of Si(111)/a–$Ni_{40}Zr_{60}$ samples annealed in oxygen ambient. 2 MeV $^4He^+$ backscattering was used. Scattering angle 115°. Sample tilt for the random spectra was 7°, channeling along the ⟨111⟩ surface normal.

Ni is released from the amorphous matrix and reacts with the underlying Si substrate. Epitaxial $NiSi_2$ is formed, as can be seen in the channeling spectrum. The ZrO_2 and the underlying $NiSi_2$ layer are very well separated, as can be seen by the sharp edges of the peaks and the shift of the Ni signal from the surface position down to lower energies. The Si signal is shifted to lower energies due to the additional stopping of the analyzing He-beam in the overlayer introduced by the oxidation reaction. From RUMP simulation we infer that the initial 400 Å thick a–$Ni_{40}Zr_{60}$ layer results in a 400 Å thick $NiSi_2$ and a 1200 Å thick ZrO_2 layer after reaction. Annealing at 600 °C results in a roughening of the surface, which is visible even by eye. Annealing at lower temperatures (down to 350 °C) or in lower oxygen pressures (10^{-6} mbar) results in the same reaction products, but the reaction proceeds much slower. This gave us the possibility of monitoring the oxidation process in more detail. It appeared that ZrO_2 oxide forms at the sample surface and the a–$Ni_{40}Zr_{60}$ remains amorphous, whereas its composition, according to RBS, shifts toward a higher Ni concentration. This has also been observed by Walz *et al.*[17] Above approximately 65 at.% Ni concentration in a–NiZr epitaxial $NiSi_2$ starts to form at the Si(111) interface with ZrO_2 on top.

The oxidation experiments show that in a one-step annealing process a well-separated bilayer structure of $NiSi_2/ZrO_2$ can be prepared, starting with a–NiZr. The $NiSi_2$ is grown epitaxially on the Si(111) substrate. The ZrO_2 is formed at the sample surface, where the oxygen is supplied. This reaction is extremely exothermic (in Ref. 14 a value of −365 kJ/mole is given for the heat of formation of ZrO_2). Comparing the heats of formation of NiO (−120 kJ/mole) and $NiSi_2$ (−30 kJ/mole), we might expect oxidation of the Ni also; however, silicidation of Ni is observed probably because ZrO_2 acts as a buffer layer under which Ni can freely react with Si.

III. CONCLUSIONS

We have shown that Ni can diffuse through a–NiZr to form epitaxial $NiSi_2$ on Si(111) at 350 °C. Also, polycrystalline $NiSi_2$ is formed by reaction of a–NiZr with a–Si at 350 °C. This is in contrast to the general observation that amorphous alloys of near noble and refractory metal atoms react with Si only at the reaction temperature of the refractory metal with Si, i.e., $\geqslant$600 °C. Amorphous Ni–Zr belongs to a special class of amorphous alloys that can be formed by a solid state reaction. The diffusion of the near noble metal in the a–NiZr is sufficient to supply Ni for $NiSi_2$ formation, yet the diffusion is slow enough to allow nucleation and growth of epitaxial layers on Si(111). Amorphous Si appears to be more reactive than crystalline Si. This is attributed to the difference in free energy of 10 to 15 kJ/mole.

Also, we have shown that annealing in oxygen ambient of Si(111)/*a*–NiZr samples results in bilayer formation of epitaxial $NiSi_2$ and polycrystalline ZrO_2.

These results may be applied to microelectronic applications for the formation of epitaxial silicides and protective buffer layers in a single annealing step at low temperatures.

ACKNOWLEDGMENTS

The authors wish to thank R. J. I. M. Koper and H. Zeijlemaker for assistance with the depositions. We are obliged to A. C. Moleman and W. F. Moolhuyzen of the University of Amsterdam for assistance and use of the x-ray equipment. Discussions with G. J. van der Kolk and J. P.W. B. Duchateau of Philips Research Laboratories in Eindhoven were most helpful and stimulating. This work is part of the research program of the Stichting voor Fundamenteel Onderzoek der Materie (Foundation for Fundamental Research on Matter) and was financially supported by the Nederlandse Organisatie voor Wetenschappelijk Onderzoek (Netherlands Organization for the Advancement of Research).

REFERENCES

[1]F.W. Saris, L. S. Hung, M. Nastasi, and J.W. Mayer, MRS Symp. Proc. **54**, 81 (1986).

[2]K. Samwer, Physics Reports **161**, 1 (1988).

[3]J. C. Barbour, Phys. Rev. Lett. **55**, 2872 (1985).

[4]B. M. Clemens, W. L. Johnson, and R. B. Schwarz, J. Non-Cryst. Solids **61–62**, 817 (1984).

[5]K. H. J. Buschow, J. Phys. F: Met. Phys. **14**, 593 (1984).

[6]Z. Altounian, Tu Guo-hua, and J. O. Strom-Olsen, J. Appl. Phys. **54**, 3111 (1983).

[7]N. Saunders and A. P. Miodownik, J. Mater. Res. **1**, 38 (1986).

[8]F. R. de Boer, R. Boom, W. C. M. Mattens, A. R. Miedema, and A. K. Niessen, *Cohesion in Alloys*, edited by F. R. de Boer and D. Pettifor (North Holland, Amsterdam, 1988).

[9]Y. T. Cheng, W. L. Johnson, and M-A. Nicolet, Appl. Phys. Lett. **47**, 800 (1985).

[10]L. R. Doolittle, Nucl. Instrum. Methods **B9**, 344 (1985).

[11]K. Hoshino, R.S. Averback, H. Hahn, and S.J. Rothman, J. Mater. Res. **3**, 55 (1988).

[12]K. N. Tu, E.I. Alessandrini, W. K. Chu, H. Krautle, and J.W. Mayer, Jpn. J. Appl. Phys. Suppl. 2, Pt. 1, 669 (1974).

[13]F. M. d'Heurle, C. S. Petersson, J. E. E. Baglin, S. J. LaPlaca, and C.Y. Wong, J. Appl. Phys. **55**, 4208 (1984).

[14]M-A. Nicolet and S. S. Lau, in *VLSI Electronics: Microstructure Science*, edited by N. G. Einspruch and G. B. Larrabee (Academic Press, New York, 1983).

[15]Q. Z. Hong, L. S. Hung, and J.W. Mayer, J. Appl. Phys. **65**, 3395 (1989).

[16]S. Roorda, S. Doorn, W. C. Sinke, P. M. L. O. Scholte, and E. van Loenen, Phys. Rev. Lett. **62**, 1880 (1989).

[17]B. Walz, P. Oelhafen, H-J. Güntherodt, and A. Baiker, Appl. Surf. Sci. **37**, 337 (1989).